Spray deposited β-Bi2O3 nanostructured films with visible photocatalytic activity for solar water treatment

Journal:	*Photochemical & Photobiological Sciences*
Manuscript ID:	PP-ART-10-2014-000367.R2
Article Type:	Paper
Date Submitted by the Author:	15-Mar-2015
Complete List of Authors:	Barrera-Mota, Karen; Universidad Nacional Autonoma de Mexico, Instituto de Investigaciones en Materiales, Bizarro, Monserrat; Universidad Nacional Autonoma de Mexico, Instituto de Investigaciones en Materiales Castellino, Micaela; Center for Space Human Robotics @Polito, Istituto Italiano di Tecnologia, Tagliaferro, Alberto; Politecnico di Torino, Department of Applied Science and Technology Hernandez-Ramirez, Aracely; Universidad Autonoma de Nuevo Leon, Facultad de Ciencias Qímicas Rodil, Sandra; Universidad Nacional Autonoma de Mexico, Instituto de Investigaciones en Materiales,

SCHOLARONE™
Manuscripts

Spray deposited β-Bi_2O_3 nanostructured films with visible photocatalytic activity for solar water treatment

Karen Barrera-Mota[1], Monserrat Bizarro[1]*, Micaela Castellino[2], Alberto Tagliaferro[3], Aracely Hernández[4], Sandra E. Rodil[1]

[1]Instituto de Investigaciones en Materiales, Universidad Nacional Autónoma de México, A.P. 70-360, Coyoacán, D.F., C.P. 04510, México.

[2]Center for Space Human Robotics @Polito, Istituto Italiano di Tecnologia, Corso Trento 21, 10129 Torino, Italy

[3]Department of Applied Science and Technology, Politecnico di Torino, Turin10129, Italy.

[4]Facultad de Ciencias Químicas, Universidad Autónoma de Nuevo León, San Nicolás de los Garza, N.L. México.

*E-mail of corresponding author: monserrat@iim.unam.mx

Abstract

Bismuth oxide thin films were obtained by spray pyrolysis method using bismuth acetate as precursor salt. The films were characterized by X-ray diffraction (XRD), Fourier Transform Infrared (FTIR), UV-vis diffuse reflectance, X-ray Photoelectron Spectroscopy (XPS) and Scanning Electron Microscopy (SEM). The XRD patterns indicated that the pure β phase is obtained at 450 °C and was also confirmed by FTIR. This phase presents a nanoplate morphology which is adequate for the photocatalytic reactions. Moreover, the band gap value was of 2.6 eV indicating a good capacity of visible light absorption. The photocatalytic degradation of the Methyl Orange (MO) dye was pH dependent, being the acid solution easier to degrade. However, the Bi_2O_3 films were easily converted into BiOCl when they were in contact with a solution containing HCl. In order to preserve the β-Bi_2O_3 phase, the Acid Blue 113 dye with its natural pH of 8 was used to evaluate the stability of the photocatalytic activity after five degradation cycles. The photoactivity

was practically stable indicating a good performance of the material. This encouraged us to test the films in a continuous flow solar reactor prototype for the degradation of the dye solution using sunlight radiation exclusively. The good performance of the β-Bi_2O_3 films indicates that they can be used for sustainable water treatment applications.

Keywords: Bismuth oxide; thin films; photocatalysis; photoreactor; sunlight.

1. Introduction

Photocatalytic water treatment technologies are of special interest nowadays, where environmental friendly and sustainable processes need to be implemented in order to keep the modern life style. The real capabilities of the process have been widely demonstrated for TiO_2 based materials[1, 2], with the disadvantage of the requirement of continuous UV light illumination that does not allow the use of natural sunlight energy. The scientific community is therefore looking for either doping/modifying the TiO_2 materials in order to enhance the visible-light response or to find other semiconductor materials with lower-than-TiO_2 band-gap energies which present comparable photocatalytic activities. One of such materials is Bismuth oxide, for which it has been shown that micrometric and nanometric powders and nanostructures have a strong potential for photocatalytic degradation of dyes (rhodamine B[3], methyl orange[4, 5], indigo carmine, methylene blue[6], malachite green[7], etc…), drugs (acetaminophen[8], tetracycline[9]), 4-chlorophenol[3, 4], acetaldehyde[10] as well as gases (toluene, NO and HCHO[11]). The use of slurry photocatalytic systems is very efficient due to the large surface active sites of the powders/nanoparticles. However, for a photoreactor a second process has to be implemented in order to recover the slurry, which increases the cost. The other option is the immobilization of the photocatalyst into an adequate support, where the difficulty resides on the attachment of the nanometric catalysts to the support. On the other hand, thin film photocatalyst could be used as a coating directly applied into the photoreactor walls, or deposited on grids through which the water can go through. The lower effective surface area obtained for thin films demands better and more efficient photocatalytic semiconductors, thus recent efforts are focused on obtaining higher surface area photocatalysts as well as visible-light active materials. One of these new promising materials in thin film form is bismuth oxide (Bi_2O_3).

Bi_2O_3 possesses six polymorphisms: α-Bi_2O_3 (monoclinic), β-Bi_2O_3 (tetragonal), γ-Bi_2O_3 (BCC), δ-Bi_2O_3 (cubic), ε-Bi_2O_3 (triclinic) and ω-Bi_2O_3 (triclinic), being this last one recently synthesized by Cornei et al.[12, 13]. The α and δ phases are stable, while β, γ, ε and ω are metastable. Among all these polymorphic forms, β-Bi_2O_3 has the strongest absorption in the visible light because it has the smallest band-gap (~2.58 eV)[14], making it a good candidate as visible light-activated photocatalyst. However, this tetragonal phase is metastable and its synthesis is not easy, especially on the nanoscale[15]. The formation of non-stoichiometric bismuth oxide phases has been also frequently reported, like the Bi_2O_3/Bi_2O_{3+x} system produced by thermal vacuum treatment reported by Sajjad et al.[16] which produced new forms of Bi creating new defect states, or the Bi_2O_3/Bi_2O_{4-x} nanocomposite reported by Hameed et al. which showed a good photocatalytic degradation of methylene blue,

methyl orange and phenol[17]. Furthermore, Bi_2O_3 is a p-type semiconductor with suitable band edge potentials for water oxidation[17-19]. As thin films, the δ-Bi_2O_3 has been obtained by electrodeposition by Koza et al.[20] and Helfen et al.[21] Oxidation processes of Bi-deposited films were applied by Leontie et al.[14] and Patil et al.[22] The Sol-Gel route has been used by Fruth et al.[23], obtaining an oxygen deficient phase, and by Xiaohong et al.[24] who showed that monoclinic and tetragonal phases could be obtained after annealing above 550 °C. Spray pyrolysis has been used by Lockhande and Bhosale[25] and Rico-Fuentes et al.[26] The latter used bismuth acetate as the source solution and obtained two bismuth oxide phases: β-Bi_2O_3 and the substoichiometry $Bi_2O_{2.33}$; this latter was converted into the β-phase after annealing. Soitah et al.[27] studied the optical and electrical properties of bismuth oxide films produced by a Pechini modified route and annealing at temperatures ranging between 400 °C and 700 °C. Physical deposition methods, such as pulsed laser deposition and magnetron sputtering have also been used[28-32]. A strong influence of the synthesis method and synthesis parameters on the Bi_2O_3 phases and their properties has been observed, and still there are many questions to answer in order to understand this compound better. In this paper, we demonstrate that it is possible to obtain a pure β-phase Bi_2O_3 film by selecting the appropriate temperature and deposition parameters of the spray pyrolysis method. We also show that this β-phase is photocatalytic active not only under UV but also using visible light; this fact motivated us to incorporate this material into a solar reactor prototype to prove its possible use in water treatment applications.

2. Experimental details

2.1 Synthesis of Bi_2O_3 films

The precursor solution was prepared using Bismuth(III) acetate $Bi(CH_3CO_2)_3$ from Sigma-Aldrich in a molar concentration of 0.05, dissolved in acetic acid 25%v and deionized water 75%v at 45 °C under constant stirring in order to obtain a transparent homogeneous solution. This solution was deposited by the pneumatic spray pyrolysis technique at temperatures of 350, 375, 400, 425 and 450 °C, in order to identify the optimum deposition temperature. For each deposition 100 mL of the solution were sprayed at a flow rate of 4 mL/min and an air flow rate of 1.13 L/min. The substrates used in this work were Corning glass slides of 2.5 cm x 1.25 cm and c-Si substrates of 1 cm x 1 cm. The former were cleaned with trichloroethylene, acetone and methanol consecutively in an ultrasonic bath and dried with compressed nitrogen. Silicon substrates were cleaned with P solution, rinsed with deionized water and dried with compressed nitrogen.

2.2 Characterization

The films were characterized by X-ray diffraction (D8 Advance Bruker) using the CuK_α wavelength (1.54056 Å). The morphology of the films was studied by Scanning Electron Microscopy (JSM-7600F Jeol). The thickness and roughness were measured with a profilometer (Sloan Dektak IIA) and Fourier Transformed Infrared (FTIR) spectra were acquired using a Nicolet 210 FTIR. The band gap of the material was determined from the diffuse reflectance spectra (DRS) acquired using a Perkin Elmer Lambda 35 UV-vis spectrophotometer equipped with an integration sphere; Spectralon® was used as reference blank. A PHI 5000 Versaprobe II Scanning X-ray Photoelectron Spectrometer (monochromatic Al K-alpha X-ray source with 1486.6 eV energy, 15 kV voltage and 1 mA anode current), was used to investigate the surface chemical composition. A spot size of 100 μm was used in order to collect the photoelectron signal for both the high resolution (HR) and the survey spectra. Different pass energy values were exploited: 187.85 eV for survey spectra and 23.5 eV for HR peaks.

2.3 Photocatalytic tests

The photocatalytic activity of the Bi_2O_3 films was evaluated by the degradation of a typical organic dye solution: either Methyl Orange (MO) dye ($C_{14}H_{14}N_3NaO_3S$) or Acid Blue 113 ($C_{32}H_{21}N_5Na_2O_6S_2$) both from Sigma-Aldrich, with a concentration of 10^{-6} M (their absorption spectra are shown in Fig. A of the Electronic Supplementary Information). The films were placed in pairs inside a vial with 10 mL of the dye solution and exposed to different light sources in order to study the effect of the energy radiation. Three light sources with different wavelength ranges were used: a UV light lamp (26 W/m^2), a white light lamp (33 W/m^2) and simulated sunlight radiation (Oriel 96000 Xenon lamp with an intensity of 397 W/m^2). The degradation was measured by following the absorbance spectrum of the dye solution each 30 min. Total Organic Carbon (TOC) measurements were obtained using a Shimadzu TOC-V CSH and High Performance Liquid Chromatography (HPLC) Perkin Elmer 600 series Link; chromatography was used to analyze the dye decomposition.

3. Results

3.1 Microstructure, morphology and composition

Fig. 1a shows the evolution of the crystalline structure of the bismuth oxide films with the deposition temperature. At low temperatures, both BiO and β-Bi_2O_3

phases were observed, as well as one peak corresponding to bismuth acetate (BiAc); this indicates that at these temperatures residues of the precursor are still present. When the temperature was increased to 450 °C, the pure β-Bi_2O_3 phase was obtained, as it is confirmed by the FTIR spectra of Fig. 1b. FTIR analysis shows the evolution of BiO_6, BiO_3 and BiO compounds with increasing temperature leading to the β-Bi_2O_3 phase at 450 ºC. This was confirmed by XRD on several repetitions of the growth of the material at 450 ºC, as shown in Fig. 1d, where the most prominent peaks correspond to the (201) and (220) families, according to the ICDD file No. 78-1793. Fig. 1c, shows the morphology of the β-Bi_2O_3 films, composed by mostly oriented nanoplates with rounded borders, with approximate dimensions of 30 x 200 nm. Such morphology is ideal for photocatalytic processes as it provides higher surface area than a flat surface.

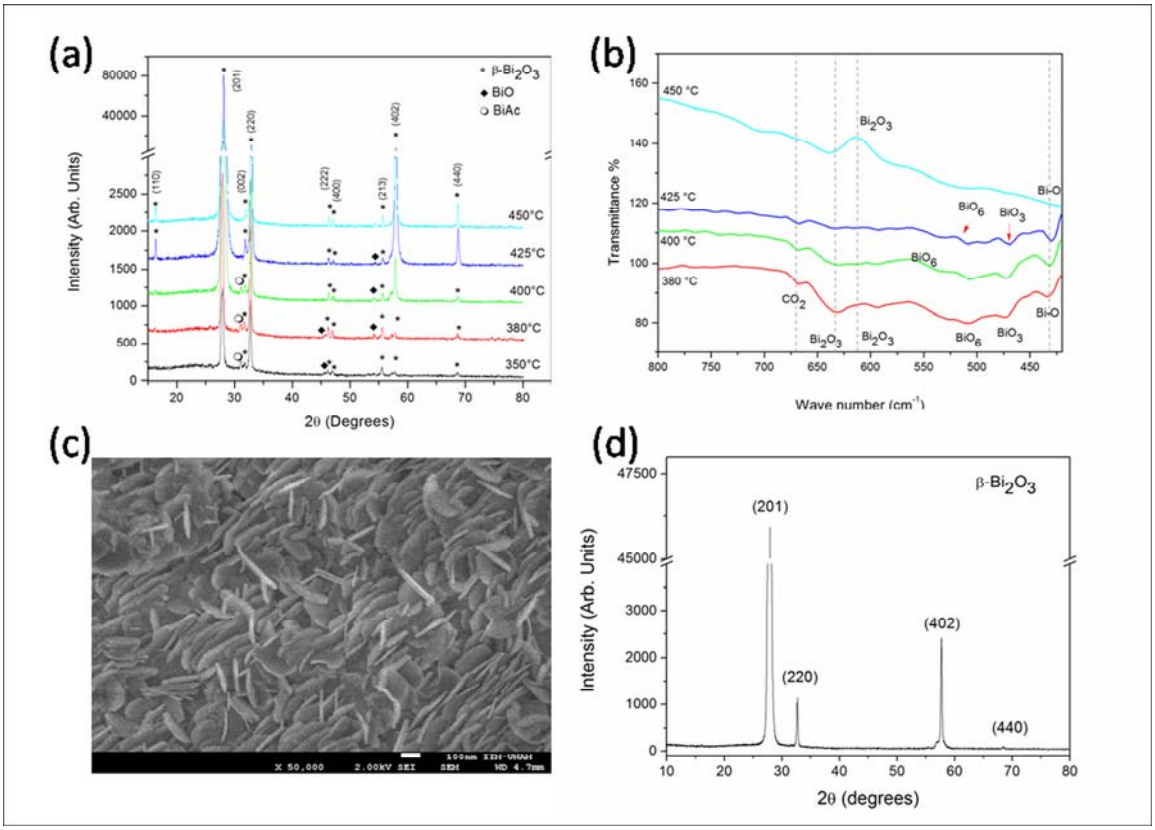

Fig. 1 (a) XRD patterns of films deposited at different temperatures, it is appreciated that BiO and BiAc peaks disappear at 450 °C. (b) FTIR spectra of the samples grown at different temperatures. (c) SEM image of the β-Bi_2O_3 film grown at 450°C with a nanoplate structure. (d) XRD pattern of the sample grown at 450 ºC, where the β-Bi_2O_3 phase is exclusively obtained.

To evaluate the composition of the films, XPS analyses of the films were performed without argon cleaning. The XPS survey spectrum (Fig. 2a) shows three main photo-electronic peaks: O1s, C1s and Bi4f; their relative atomic concentrations were evaluated after subtracting the background using a Shirley function[33] obtaining a relative atomic composition of 49.2% of C, 37.7% of O and 13.1% of Bi. The carbon signal is coming from adventitious carbon, *i.e.* carbon species adsorbed on the semiconductor surface as a consequence of the exposition of the sample to atmospheric conditions. High resolution (HR) spectra of these peaks were acquired in order to evaluate the chemical bonding state. After an exhaustive research in literature[34,35] the peaks were attributed to different chemical species. The C1s peak is made up by three bonds: a first peak at lower binding energy due to C-C/C-H, a small shoulder due to C-O and a well-separated third peak due to C=O[36]. The O1s peak is also made up by three components: two of them due to the bonds with C and a bigger one at higher energy due to Bi oxide. Bi4f doublet peak ($Bi4f_{7/2}$ and $Bi4f_{5/2}$) is made up by the superposition of two peaks each: the first at 156.8 eV assigned to metallic Bi[37] and the second one at 158.5 eV assigned to Bi_2O_3 (the same two peaks are present also in the $Bi4f_{5/2}$ separated by a Δ=5.4 eV).

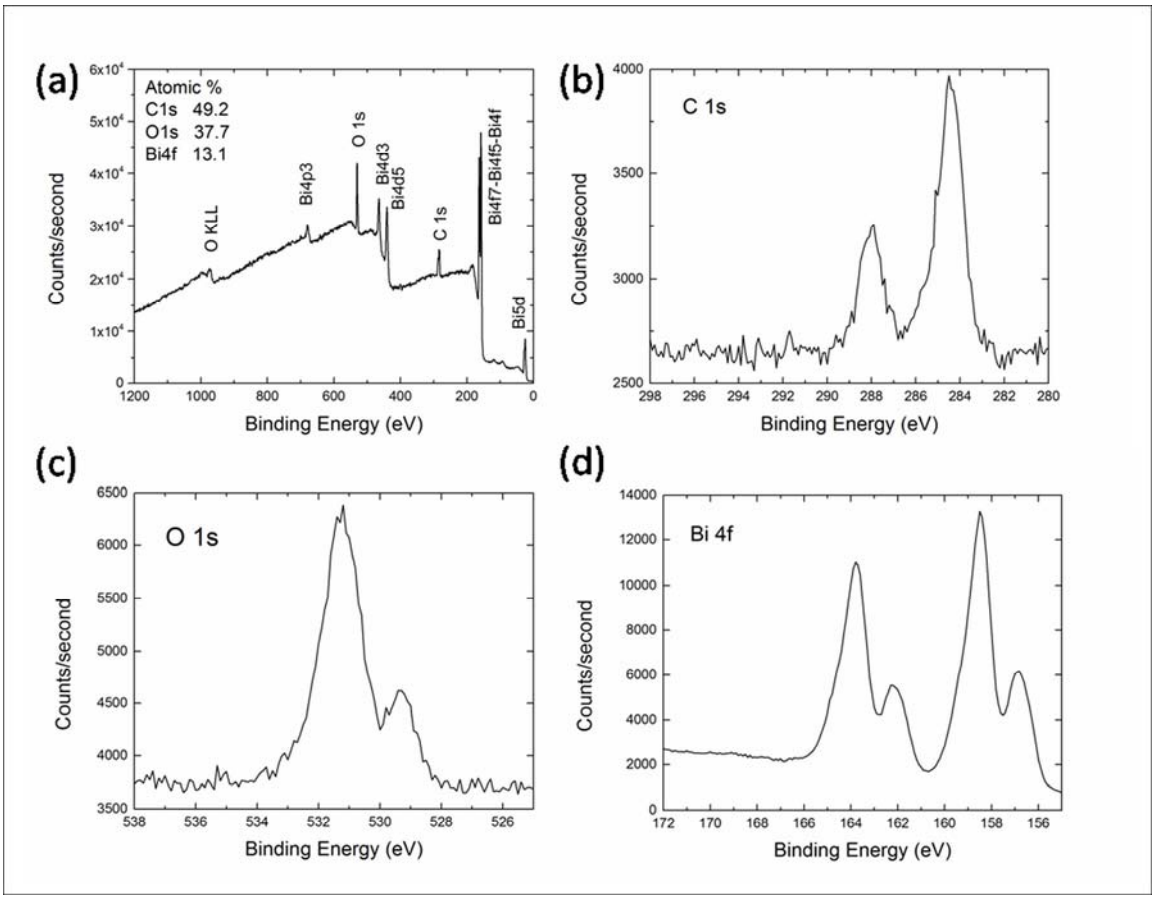

Fig. 2 XPS analysis of Bi_2O_3 films. (a) survey spectrum, (b) C1s, (c) O1s, (d) Bi 4f high resolution spectra.

3.2 Optical properties

The optical properties of the films were evaluated by their UV-vis reflectance spectra. To convert the diffuse reflectance to the absorption coefficient α the Kubelka-Munk function *F(R)* was calculated as shown in eq. 1; then $[F(R)*E]^2$ was plotted against the energy *E* and the extrapolation of the linear fitting to its intersection with the abscissas determined the band gap energy E_g, as can be seen in Fig. 3.

$$\alpha \approx \frac{(1-R_\infty)^2}{2R_\infty} \equiv F(R_\infty) \qquad \text{(Eq. 1)}$$

The band gap of all the β-Bi_2O_3 films was determined giving an average value of 2.60 $\pm$ 0.07 eV, indicating a good agreement with the reported values for this

phase[38]. This band gap value causes the material to absorb light of wavelengths down to 477 nm or in the blue region of the visible spectrum.

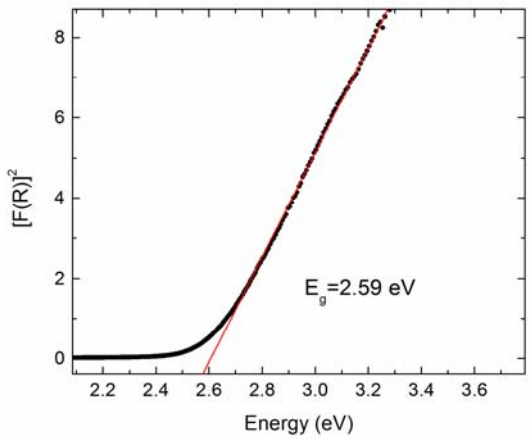

Fig. 3 Example of the determination of the energy band gap by means of the Kubelka-Munk function.

3.3 Photocatalysis

The photocatalytic activity of the β-Bi_2O_3 films was initially tested on the degradation of the methyl orange dye. The first tests indicated that the photocatalytic activity was highly pH-dependent, showing the highest degradation for the lowest pH values, as presented in figure 4a. This may be due to the specific form of the MO molecule in acid or basic environment[39] (insets of fig. 4a). As the degradation of the dye solution at neutral pH was very low we decided to evaluate the photocatalytic activity of the films under acidic conditions (pH=3). In this case, a good photocatalytic performance of the β-Bi_2O_3 was observed, achieving more than 80% of discoloration of the dye after 180 min (Fig. 4b), as it can be seen in the change of the absorption spectrum of the dye (bottom inset of figure 4b). The kinetics analysis revealed a first order reaction (top inset of fig. 4b), with an apparent rate of reaction $k=9.5x10^{-3}$ min^{-1}. Some reports related to the use of immobilized catalysts as thin layers, describe the degradation reaction of organic pollutants with the Langmuir-Hinshelwood kinetic model [40, 41] and the mass transfer effect has been found to be negligible in some cases[42], but this has to be verified in each specific reactor configuration. As it was previously mentioned, the band gap of the β-Bi_2O_3 films was of 2.6 eV, which means that it is able to absorb visible light starting from wavelengths of 477 nm. In order to prove this, three equivalent films were tested under different illumination sources: (i) simulated sunlight, (ii) white

light, and (iii) UV light again to compare; the emission spectra of each lamp was reported previously[43]. Figure 4c shows the performance of the films under these three irradiation sources, where is remarkable the highest efficiency of the films under sunlight achieving the complete discoloration in 180 minutes. The sample exposed to UV light degraded 80% of the dye, whereas the sample exposed to white light only reached about 60% in the same time. The high degradation efficiency of the sample exposed to simulated sunlight is attributed to the intensity of the lamp, which was higher than that used for the other two lamps. However, a degradation of 60% of the dye using white light is particularly noteworthy when compared to TiO_2 ─the widest used photocatalyst─ which is only activated by UV light. Just as a reference for comparison purposes, in a previous work TiO_2 films with different surface morphologies were produced by spray pyrolysis and tested under similar conditions, illuminating only with UV light[44]. The TiO_2 films modified with P25 powder supported on the surface presented a rate of reaction of 0.0069 min^{-1}, while the pure TiO_2 P25 powder had a value of 0.02 min^{-1}. In the present case, the β-Bi_2O_3 films showed a rate of reaction of 0.0095 min^{-1} under UV light, which is still nearly half the value of the P25 powder. Nonetheless compared to the TiO_2 films, the β-Bi_2O_3 films presented a higher reaction rate. This result is encouraging especially because bismuth oxide is able to absorb visible light.

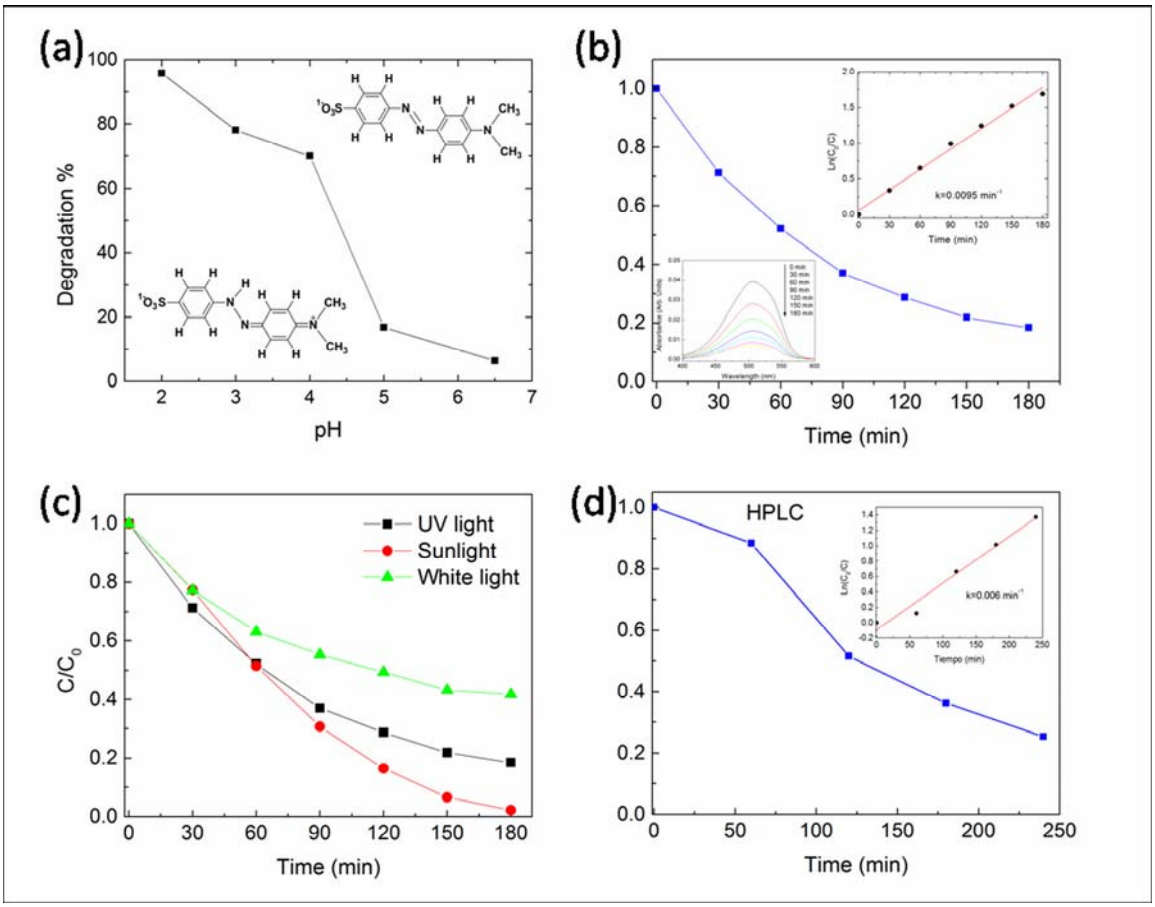

Figure 4. (a) pH dependence of the MO degradation with β-Bi_2O_3 films. (b) Photocatalytic degradation of the dye during time. The inset at the bottom shows the change of the absorption spectrum of the dye; the inset at the top shows a first order reaction rate. (c) Effect of different illumination sources on the photocatalytic degradation of the MO dye. (d) Degradation of the MO dye followed by HPLC technique; the inset shows a linear kinetic of the reaction.

HPLC is a very precise technique to measure the concentration of the dye solution and determine its degradation. This technique was used to analyze the degradation of the MO solution with a 10^{-5} M concentration exposed to direct sunlight and using the β-Bi_2O_3 films. It is important to remark that the higher the concentration, the slower the reaction occurs; however, the evolution of the concentration of the dye solution was good, reaching a 70% of degradation in 4 hours (with a k=6x10^{-3} min^{-1}) as shown in figure 4b. The total organic carbon (TOC) was also measured before and after the degradation test. The obtained values were $TOC_{initial}$=2.599 mg/L, TOC_{final}=1.680 mg/L, which means that the photocatalyst mineralized 35% of the dye (0.919 mg/L). It is important to remark

this issue, because even though we can have a transparent solution after the degradation process, the complete mineralization is not yet achieved. More time is required to complete the necessary reactions to get water free of contaminants.

The stability of the photocatalytic activity of the films was evaluated by repeating the degradation experiments reusing the same films. Fig. 5a indicates that the photocatalytic efficiency remained practically constant after five degradation cycles of the MO dye under simulated sunlight. However, after the fifth cycle, a change in the color of the film was noticed (from a light yellow to a white color), indicating a modification of the composition of the film. XRD analysis was performed on this sample after the treatment, revealing the presence of only BiOCl, as shown in Fig. 5b. The reason of this transformation is that the β-Bi_2O_3 film was in contact with a solution that contained HCl to reduce the pH, reacting as follows:

$$Bi_2O_3 + 2HCl \rightarrow 2BiOCl + H_2O$$

Considering the Gibbs energy of the products minus the Gibbs energy of the reactants at 298 K, the energy of the reaction is:

$$\Delta E = 2\Delta G_f^0(BiOCl) + \Delta G_f^0(H_2O) - \Delta G_f^0(Bi_2O_3) - 2G_f^0(HCl)$$

$$= 2(-322.17\ \mathrm{kJ/mol}) + (-228.59\ \mathrm{kJ/mol}) - (-493.71\ \mathrm{kJ/mol}) - 2(-95.31\ \mathrm{kJ/mol})$$

$$= -569.84\ \mathrm{kJ/mol}$$

This indicates that the reaction is favorable. In order to avoid the transformation of β-Bi_2O_3 to BiOCl, a different dye was tested without the addition of acid. For this experiment Acid Blue 113 dye was used leaving the solution with its original pH value of 8. Two different concentrations (10^{-6} and 10^{-5} M) were tested under simulated sunlight, achieving 71.7 and 59.2% of dye degradation, respectively (Fig. 5c). The decrease of the degradation rate is due to the higher number of dye molecules in the solution that must adsorb into the film's surface, then react, desorb and incorporate again into the liquid in order to continue the process. Nonetheless, the degradation is only slightly lower although the concentration is 10 times larger. The total organic carbon of the Acid Blue 113 dye was measured before and after the photocatalytic process and the values were $TOC_{initial}$=3.429 mg/L and TOC_{final}=2.425 mg/L, indicating a mineralization of 29.3% of the dye. This response suggested that the β-Bi_2O_3 films could be used in a solar photocatalytic reactor prototype in order to scale up the system for possible use in water treatment. The analysis of the adsorption of the dye onto the film's surface before the illumination showed that the Acid Blue 113 dye adsorbed more onto the Bi_2O_3 film (~16%) than the methyl orange dye (negligible), as can be seen in Fig. B of the Electronic Supplementary Information.

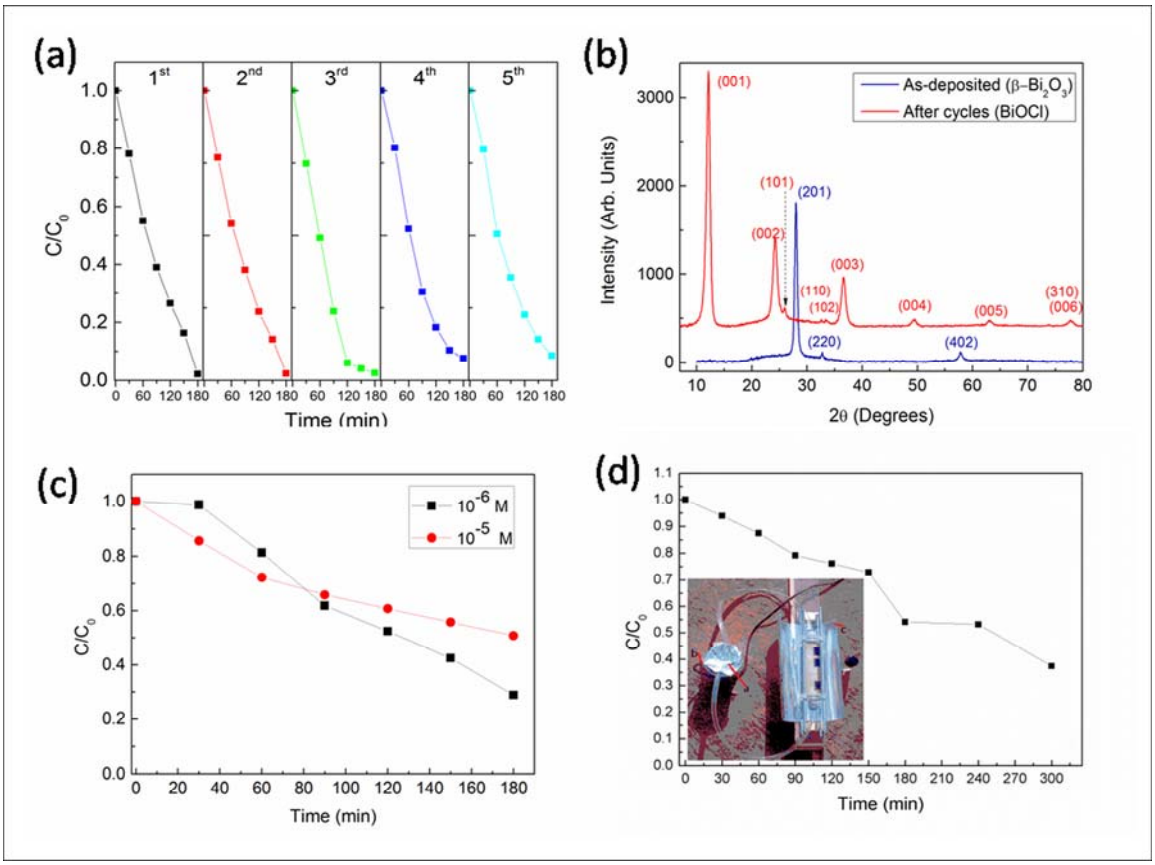

Fig. 5 (a) Degradation test under simulated sunlight after five cycles; the efficiency of the films remains practically constant. (b) XRD of as-deposited β-Bi_2O_3 film and after 5 degradation cycles, where it transformed to BiOCl. (c) Degradation of acid blue 113 at two different concentrations. (d) Dye degradation performance of the β-Bi_2O_3 films using a CPC solar reactor.

For this purpose, a small scale home-made Compound Parabolic Collector (CPC) solar reactor was implemented, and it is shown in Fig. 6; Fig. 6a shows the diagram of a cross section view of the reactor, and Fig. 6b is a picture of the prototype. Ten photocatalytic films with a total area of 62.5 cm^2 were placed along the axis of the reactor tube and the dye solution was pumped through it at a rate of 10 mL/s. The CPC has an acceptance angle of 90º and the total volume of treated solution was 230 mL. With this configuration a 46% of dye discoloration was obtained in 3 hours, and 62% letting the reaction for a total of 5 hours, as shown in Fig. 5d. This result indicates a good performance of the material under ambient conditions. The smaller degradation percentage observed in the solar reactor

compared to the experiments performed in the glass vials is due to the larger solution volume to film's surface ratio (V_{sol}/A_{film}), as can be seen in Table 1. Although an improvement of the V_{sol}/A_{film} as well as of the whole experimental setup can be done, these results show a promising performance of the β-Bi_2O_3 films for sustainable and environmentally friendly water treatment processes.

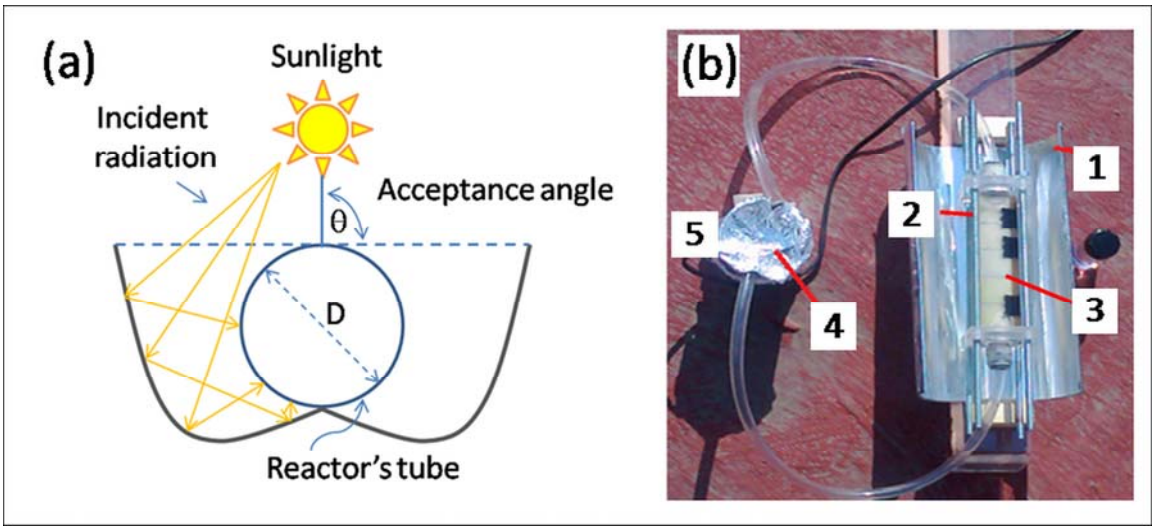

Fig. 6 (a) Diagram of the cross section of the CPC solar photocatalytic reactor, where the acceptance angle is θ=90° and the diameter is D=3.05 cm. (b) Prototype of the solar reactor, where (1) is the collector, (2) is the reactor's tube, (3) are the thin films, (4) mixing tank, (5) water pump.

Table 1. Comparison of the photocatalytic performance of the β-Bi_2O_3 films in the lab scale reactor and the CPC solar reactor, using Acid Blue 113 dye at 10^{-6}M.

Type of reactor	Degradation %	Reaction time (min)	Solution volume (mL)	Area of photocatalyst (cm^2)	V_{sol}/A_{film}
CPC solar reactor	45.9	180	230	62.5	3.7
Glass vials	71.7	180	10	3.6	2.8

4. Discussion

The spray pyrolysis technique allowed the growth of pure β-phase Bi_2O_3 films at 450 ºC that presented good photocatalytic activity in specific conditions. However, at the present stage it would be crude and misleading to compare the performance of Bi_2O_3 films directly with TiO_2. More studies are needed to understand the processes involved with β-Bi_2O_3 photocatalyst. As it is often claimed, there are several factors that affect the photocatalytic reactions. Friedmann et al. classified these parameters into intrinsic –related directly with the semiconductor, such as crystallographic phase, crystallite size, impurities, etc.– and extrinsic –that involve the surrounding environment and conditions, including pH of the solution, structure of the pollutant, its initial concentration, light intensity, among others–[45]; however, all of these parameters may affect in different way for different systems (defining a system as the couple of photocatalyst and pollutant). It is not evident that one specific parameter will give the same contribution in all systems. Certain correlations have been found in the well known TiO_2, but for the new photocatalysts such as Bi_2O_3 these contributions may not be the same. In our work, the extrinsic parameters were evident in the case of the photocatalytic treatment of methyl orange because pH was decisive in the degradation percentage achieved by the films, as exposed in figure 4a. The other parameter that could affect is the light intensity in the case of the simulated sunlight, giving a higher discoloration percentage compared to the UV light while keeping the rest of the parameters constant (Fig. 4c). Here is worth to comment that for a photocatalyst in the thin film form the photoactive area is the one that is completely exposed on the surface. This means that even though the material is porous or rough, most of the photons cannot reach the deeper or more hidden parts of it and they will not contribute to the reactions. Roughness becomes important in the micrometer regime, while very low values of it do not play such a relevant role. In our Bi_2O_3 films the surface is formed by compacted nanoplates, with an average roughness of 60 nm. This roughness increases the surface area compared to a smooth film, but their compact structure avoid the formation of pores. These morphological characteristics favored the photocatalytic reactions in our system (β-Bi_2O_3 – dye). On the other hand, diffusion of the species also control the process if the rate of adsorption of the dye molecules from fluid phase is slower than the rate of electron-hole reactions with the dye molecules[46]. In addition, when the surface coverage increases, there is a slowing down of the adsorption, as observed in Fig. 5c. For these reasons, in thin film photocatalysts the degradation percentage is not linearly proportional to the surface area, mainly because the internal structure remains in dark.

Dye discoloration tests provide a quick way to evaluate the photocatalytic activity of a semiconductor by the use of a UV-vis spectrophotometer; however they cannot be used as standards because the complete discoloration of the dye does not mean that the dye was degraded into innocuous compounds[47]. Then, additional tests, such as TOC, are required to verify the mineralization of the dye. This was reported by Vautier et al. for indigo carmine dye, which was mineralized by UV-irradiated TiO_2, but the color also disappeared when only using visible light; however, its TOC remained intact[48]. The dyes used in the present work (methyl orange and acid blue 113) are very stable upon illumination, so the photolysis was very low (less than 10%, as it is shown in Fig. A of the Electronic Supplementary Information), but the TOC at the end of the photocatalytic test was lower than the initial value, indicating not only a discoloration of the dye but also a true degradation, 35% in the case of MO and 29% in the case of AB113. Other aspect that sometimes discourages the test with dyes is that their degradation mechanism is complicated and the real quantum efficiency of the photocatalytic reaction cannot be easily determined. Even so, other authors are devoted to find the degradation mechanisms of this kind of compounds and their degradation byproducts[49, 50], which are important to know due to their environmental impact.

Beyond these technical issues, the degradation tests performed in this work demonstrated the effectiveness of β-Bi_2O_3 films for the degradation of diluted dyes, which is still a global major concern. Moreover, this semiconductor can be used with visible light, making it suitable for solar applications as demonstrated with our small scale CPC solar reactor.

4. Conclusions

Single β-phase Bi_2O_3 films with good photocatalytic activity can be obtained by the spray pyrolysis technique at 450 ºC. The energy band gap of 2.6 eV allows the absorption of visible light for the photocatalytic reactions and the platelet morphology is also helpful for this purpose. The activity of the films remains constant after 5 degradation cycles; however, if the solution contains HCl the chlorine reacts with the Bi_2O_3 forming BiOCl, which indeed is also a photocatalyst. The good performance of the β-Bi_2O_3 films under direct sunlight exposure is strong evidence that this material can be used for water treatment in solar reactors.

Acknowledgements

The authors fully acknowledge M.Sc. Adriana Tejeda and Dr. Omar Novelo for their technical assistance. The research leading to these results has received funding from the European Community Seven Framework Programme (FP7-NMP-2010-EU-MEXICO) and CONACYT under grant agreements 263878 and 125141; from the PHOCSCLEEN project (FP7-PEOPLE-2012-IRSES reference 318977) and CIC-UNAM (COIC-STIA-236-14); from CONACYT- Redes Temáticas under grant No. 193883 and from PAPIIT-UNAM IB101912-RR181912 and IN106015.

References

1. H. Xu, S. Ouyang, L. Liu, P. Reunchan, N. Umezawa and J. Ye, Recent advances in TiO2-based photocatalysis, *Journal of Materials Chemistry A*, 2014, **2**, 12642-12661.
2. T. Zhang, X. Wang and X. Zhang, Recent Progress in TiO2-Mediated Solar Photocatalysis for Industrial Wastewater Treatment, *International Journal of Photoenergy*, 2014, **2014**, 12.
3. M. Schlesinger, M. Weber, S. Schulze, M. Hietschold and M. Mehring, Metastable β-Bi2O3 Nanoparticles with Potential for Photocatalytic Water Purification Using Visible Light Irradiation, *ChemistryOpen*, 2013, **2**, 146-155.
4. H. F. Cheng, B. B. Huang, J. B. Lu, Z. Y. Wang, B. Xu, X. Y. Qin, X. Y. Zhang and Y. Dai, Synergistic effect of crystal and electronic structures on the visible-light-driven photocatalytic performances of Bi2O3 polymorphs, *Phys Chem Chem Phys*, 2010, **12**, 15468-15475.
5. S. Iyyapushpam, S. T. Nishanthi and D. Pathinettam Padiyan, Photocatalytic degradation of methyl orange using α-Bi2O3 prepared without surfactant, *Journal of Alloys and Compounds*, 2013, **563**, 104-107.
6. X. Liu, L. Pan, J. Li, K. Yu and Z. Sun, Visible Light-Induced Photocatalytic Activity of Bi2O3 Prepared via Microwave-Assisted Method, *Journal of Nanoscience and Nanotechnology*, 2013, **13**, 5044-5047.
7. P. Malathy, K. Vignesh, M. Rajarajan and A. Suganthi, Enhanced photocatalytic performance of transition metal doped Bi2O3 nanoparticles under visible light irradiation, *Ceram Int*, 2014, **40**, 101-107.
8. X. Xiao, R. Hu, C. Liu, C. Xing, C. Qian, X. Zuo, J. Nan and L. Wang, Facile large-scale synthesis of β-Bi2O3 nanospheres as a highly efficient photocatalyst for the degradation of acetaminophen under visible light irradiation, *Applied Catalysis B: Environmental*, 2013, **140–141**, 433-443.
9. R. Hao, X. Xiao, X. Zuo, J. Nan and W. Zhang, Efficient adsorption and visible-light photocatalytic degradation of tetracycline hydrochloride using mesoporous BiOI microspheres, *J Hazard Mater*, 2012, **209-210**, 137-145.
10. F. Amano, K. Nogami and B. Ohtani, Enhanced photocatalytic activity of bismuth-tungsten mixed oxides for oxidative decomposition of acetaldehyde under visible light irradiation, *Catalysis Communications*, 2012, **20**, 12-16.
11. Z. Ai, Y. Huang, S. Lee and L. Zhang, Monoclinic α-Bi2O3 photocatalyst for efficient removal of gaseous NO and HCHO under visible light irradiation, *Journal of Alloys and Compounds*, 2011, **509**, 2044-2049.

12. J. Salazar-Perez, M. A. Camacho-Lopez, R. A. Morales-Luckie, V. Sánchez-Mendieta, F. Ureña-Nuñez and J. Arenas-Alatorre, Structural evolution of Bi2O3 prepared by thermal oxidation of bismuth nano-particles, *Superficies y Vacío*, 2005, **18**, 5.
13. N. Cornei, N. Tancret, F. Abraham and O. Mentré, New ε-Bi2O3 Metastable Polymorph, *Inorganic Chemistry*, 2006, **45**, 4886-4888.
14. L. Leontie, M. Caraman, M. Delibaş and G. I. Rusu, Optical properties of bismuth trioxide thin films, *Materials Research Bulletin*, 2001, **36**, 1629-1637.
15. K. Brezesinski, R. Ostermann, P. Hartmann, J. Perlich and T. Brezesinski, Exceptional Photocatalytic Activity of Ordered Mesoporous β-Bi2O3 Thin Films and Electrospun Nanofiber Mats, *Chemistry of Materials*, 2010, **22**, 3079-3085.
16. S. Sajjad, S. A. K. Leghari and J. Zhang, Nonstoichiometric Bi2O3: Efficient visible light photocatalyst, *RSC Advances*, 2013, **3**, 1363-1367.
17. A. Hameed, T. Montini, V. Gombac and P. Fornasiero, Surface Phases and Photocatalytic Activity Correlation of Bi2O3/Bi2O4-x Nanocomposite, *J Am Chem Soc*, 2008, **130**, 9658-9659.
18. M.-S. Gui, W.-D. Zhang, Q.-X. Su and C.-H. Chen, Preparation and visible light photocatalytic activity of Bi2O3/Bi2WO6 heterojunction photocatalysts, *Journal of Solid State Chemistry*, 2011, **184**, 1977-1982.
19. Y. Xu and M. A. A. Schoonen, The absolute energy positions of conduction adn valence bands of selected semiconducting minerals, *American Mineralogist*, 2000, **85**, 14.
20. J. A. Koza, E. W. Bohannan and J. A. Switzer, Superconducting Filaments Formed During Nonvolatile Resistance Switching in Electrodeposited δ-Bi2O3, *ACS Nano*, 2013, **7**, 9940-9946.
21. A. Helfen, S. Merkourakis, G. Wang, M. G. Walls, E. Roy, K. Yu-Zhang and Y. Leprince-Wang, Structure and stability studies of electrodeposited δ-Bi2O3, *Solid State Ionics*, 2005, **176**, 629-633.
22. M. M. Patil, V. V. Deshpande, S. R. Dhage and V. Ravi, Synthesis of bismuth oxide nanoparticles at 100 °C, *Mater Lett*, 2005, **59**, 2523-2525.
23. V. Fruth, M. Popa, D. Berger, R. Ramer, A. Gartner, A. Ciulei and A. Zaharescu, Deposition and characterisation of bismuth oxide thin films, *Journal of the European Ceramic Society*, 2005, **25**, 2171-2174.
24. W. Xiaohong, Q. Wei and H. Weidong, Thin bismuth oxide films prepared through the sol–gel method as photocatalyst, *Journal of Molecular Catalysis A: Chemical*, 2007, **261**, 167-171.
25. C. D. Lokhande and C. H. Bhosale, Characterisation of chemically converted sprayed Bi2O3 to Bi2S3 thin films, *Mater Chem Phys*, 1997, **49**, 46-49.
26. O. Rico-Fuentes, E. Sánchez-Aguilera, C. Velasquez, R. Ortega-Alvarado, J. C. Alonso and A. Ortiz, Characterization of spray deposited bismuth oxide thin films and their thermal conversion to bismuth silicate, *Thin Solid Films*, 2005, **478**, 96-102.
27. T. N. Soitah, Y. Chunhui, Y. Yong, N. Yinghua and S. Liang, Properties of Bi2O3 thin films prepared via a modified Pechini route, *Current Applied Physics*, 2010, **10**, 1372-1377.
28. L. Leontie, M. Caraman, A. Visinoiu and G. I. Rusu, On the optical properties of bismuth oxide thin films prepared by pulsed laser deposition, *Thin Solid Films*, 2005, **473**, 230-235.
29. L. Leontie, M. Caraman, I. Evtodiev, E. Cuculescu and A. Mija, Optical properties of bismuth oxide thin films prepared by reactive d.c. magnetron sputtering onto p-GaSe (Cu), *physica status solidi (a)*, 2008, **205**, 2052-2056.

30. H. T. Fan, S. S. Pan, X. M. Teng, C. Ye, G. H. Li and L. D. Zhang, delta-Bi2O3 thin films prepared by reactive sputtering: Fabrication and characterization, *Thin Solid Films*, 2006, **513**, 142-147.
31. P. Lunca Popa, S. Sønderby, S. Kerdsongpanya, J. Lu, N. Bonanos and P. Eklund, Highly oriented δ-Bi2O3 thin films stable at room temperature synthesized by reactive magnetron sputtering, *Journal of Applied Physics*, 2013, **113**, -.
32. B. Sirota, J. Reyes-Cuellar, P. Kohli, L. Wang, M. E. McCarroll and S. M. Aouadi, Bismuth oxide photocatalytic nanostructures produced by magnetron sputtering deposition, *Thin Solid Films*, 2012, **520**, 6118-6123.
33. D. A. Shirley, High-Resolution X-Ray Photoemission Spectrum of the Valence Bands of Gold, *Physical Review B*, 1972, **5**, 4709-4714.
34. C. Wang, C. Shao, Y. Liu and L. Zhang, Photocatalytic properties BiOCl and Bi2O3 nanofibers prepared by electrospinning, *Scripta Materialia*, 2008, **59**, 332-335.
35. V. Simon, M. Todea, A. F. Takács, M. Neumann and S. Simon, XPS study on silica–bismuthate glasses and glass ceramics, *Solid State Communications*, 2007, **141**, 42-47.
36. P. Jagdale, M. Castellino, F. Marrec, S. E. Rodil and A. Tagliaferro, Nano sized bismuth oxy chloride by metal organic chemical vapour deposition, *Appl Surf Sci*, 2014, **303**, 250-254.
37. R. Malakooti, L. Cademartiri, Y. Akçakir, S. Petrov, A. Migliori and G. A. Ozin, Shape-Controlled Bi2S3 Nanocrystals and Their Plasma Polymerization into Flexible Films, *Adv Mater*, 2006, **18**, 2189-2194.
38. L. Leontie, M. Caraman, M. Alexe and C. Harnagea, Structural and optical characteristics of bismuth oxide thin films, *Surf Sci*, 2002, **507**, 480-485.
39. A. La Rosa Toro and M. Ponce Vargas, Evaluación de electrodos de espinela de cobalto y de dióxido de plomo en la oxidación electroquímica de colorantes azo, *Revista de la Sociedad Química del Perú*, 2007, **73**, 14.
40. T. A. McMurray, J. A. Byrne, P. S. M. Dunlop, J. G. M. Winkelman, B. R. Eggins and E. T. McAdams, Intrinsic kinetics of photocatalytic oxidation of formic and oxalic acid on immobilised TiO2 films, *Applied Catalysis A: General*, 2004, **262**, 105-110.
41. J. Dostanić, B. Grbić, N. Radić, S. Stojadinović, R. Vasilić and Z. Vuković, Preparation and photocatalyic properties of TiO2-P25 film prepared by spray pyrolysis method, *Appl Surf Sci*, 2013, **274**, 321-327.
42. V. Rodgher, J. Moreira, H. de Lasa and B. Serrano, Photocatalytic degradation of malic acid using a thin coated TiO2-film: Insights on the mechanism of photocatalysis, *AIChE Journal*, 2014, **60**, 3286-3299.
43. P. Pradhan, J. C. Alonso and M. Bizarro, Photocatalytic Performance of ZnO: Al Films under Different Light Sources, *International Journal of Photoenergy*, 2012, **2012**, 7.
44. M. Bizarro, M. A. Tapia-Rodríguez, M. L. Ojeda, J. C. Alonso and A. Ortiz, Photocatalytic activity enhancement of TiO2 films by micro and nano-structured surface modification, *Appl Surf Sci*, 2009, **255**, 6274-6278.
45. D. Friedmann, C. Mendive and D. Bahnemann, TiO2 for water treatment: Parameters affecting the kinetics and mechanisms of photocatalysis, *Applied Catalysis B: Environmental*, 2010, **99**, 398-406.
46. U. I. Gaya, *Heterogeneous Photocatalysis Using Inorganic Semiconductor Solids*, Springer, 2014.
47. J. M. Herrmann, Fundamentals and misconceptions in photocatalysis, *J Photoch Photobio A*, 2010, **216**, 85-93.
48. M. Vautier, C. Guillard and J.-M. Herrmann, Photocatalytic Degradation of Dyes in Water: Case Study of Indigo and of Indigo Carmine, *J Catal*, 2001, **201**, 46-59.

49. K. Dai, H. Chen, T. Peng, D. Ke and H. Yi, Photocatalytic degradation of methyl orange in aqueous suspension of mesoporous titania nanoparticles, *Chemosphere*, 2007, **69**, 1361-1367.
50. C. Baiocchi, M. C. Brussino, E. Pramauro, A. B. Prevot, L. Palmisano and G. Marcì, Characterization of methyl orange and its photocatalytic degradation products by HPLC/UV–VIS diode array and atmospheric pressure ionization quadrupole ion trap mass spectrometry, *International Journal of Mass Spectrometry*, 2002, **214**, 247-256.